© 2003 The Chemical Society of Japan

Laser Heating Dynamics of Poly(methyl methacrylate) Films Doped with Aromatic Molecules as Revealed by Analysis of Diffusion of Triplet States

Hisashi Fujiwara,* Hiroshi Ishii, Takashi Ishiwata, Takashi Hayashi,† Hiroshi Fukumura,†,# and Hiroshi Masuhara†

Faculty of Information Sciences, Hiroshima City University, Hiroshima 731-3194

†Department of Applied Physics, Osaka University, Suita 565-0871

(Received October 15, 2002)

The 248 nm laser heating dynamics of poly(methyl methacrylate) (PMMA) doped with biphenyl or *p*-terphenyl was studied quantitatively by the analysis of temperature-dependent T_1-T_1 annihilation, which is a result of the thermally-activated diffusion of the dopants. The values of the second-order rate constant k_2 (M^{-1} s^{-1}) for the annihilation were obtained at several temperatures (293–363 K) under weak laser excitation (2–4 mJ cm^{-2}). Arrhenius plots of k_2 for both films resulted in straight lines that were used to estimate the rate constant at higher temperatures for the simulation of T_1-T_1 annihilation. Under intense excitation (100–190 mJ cm^{-2}), the T_1 decays of both films occurred faster with increased laser fluence. The comparison between these observed T_1 decays and the simulated ones revealed the following: (1) most of the absorbed photon energy, at least 70%, is used to increase the temperature of the polymer, (2) the cooling of the polymer, mainly due to heat transfer into the quartz substrate, slows down the diffusion of the dopants and, accordingly, the T_1-T_1 annihilation, and (3) the temperature at the polymer-quartz interface after laser excitation remains almost constant up to at least a few microseconds.

In recent years, we have studied a novel and interesting phenomenon: a dopant in a polymer can absorb several UV or vis photons during nanosecond laser excitation.[1–7] The existence of such multiphoton absorption was first suggested by a time-of-flight mass spectroscopic experiment on a 351 nm ablation of anthracene-doped poly(methyl methacrylate) (PMMA).[1] Later, the multiphoton absorption was confirmed for PMMA doped with biphenyl or pyrene by directly monitoring the transmitted excitation laser pulse.[3,5]

In the near-IR region (1064 nm), prior to our work, Dlott et al. had confirmed that a near-IR dye, IR-165, in PMMA can absorb several tens of photons even with a 25-ps pulse.[8–11] They attributed the multiphoton absorption to the absorption and quite efficient internal conversion between S_0 and S_1 states.[8] In general (especially with UV or vis excitation), large energy gap between both states results in inefficient $S_1 \rightarrow S_0$ internal conversion, and thus it is quite difficult to expect this type of multiphoton absorption for other molecules, except for a few exceptional cases (e.g. azulene).[12]

On the other hand, we have found multiphoton absorption for the following dopants: anthracenes,[1,2] biphenyl,[3] pyrene,[3,5] 5-diazo Meldrum's acid,[4] porphyrins,[6] and *N*,*N*,*N*′,*N*′-tetramethyl-*p*-phenylenediamine (TMPD).[7] To explain this finding we have proposed the "cyclic multiphotonic absorption" mechanism (Fig. 1), where dopant transients work as repetitive absorbers of laser photons.[1,2] Intense excitation of a dopant, which is initially in the ground state (G), should result in the dense formation of transient states (A), such as the lowest excited singlet (S_1) and triplet (T_1) states, cations, and anions.

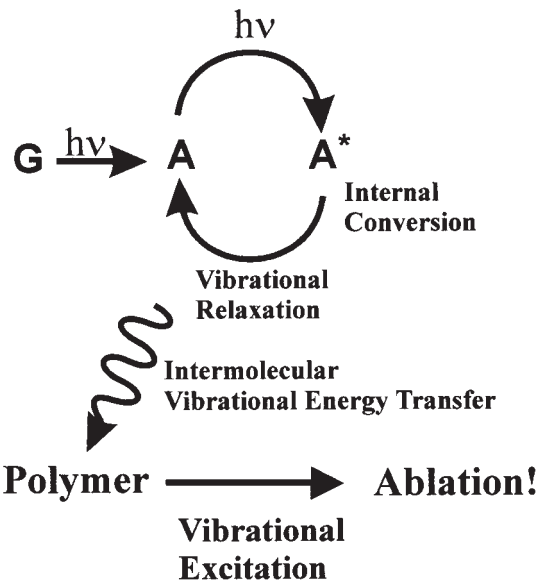

Fig. 1. Schematic representation of the cyclic multiphotonic absorption mechanism. The symbol **G** represents the ground state of a dopant. The symbols **A** and **A*** represent transient states of a dopant and their excited states respectively.

Present address: Department of Chemistry, Tohoku University, Sendai 980-8577

The higher excited states (A^*, e.g. S_n, T_n, and excited states of ions), which are produced by the successive absorption of excitation photons, generally have a lifetime much shorter than the duration of a nanosecond laser pulse. The rapid relaxation of those states to the original transient states allows for the cyclic absorption of excitation photons. This mechanism can apply to molecules whose transient states have substantial absorption coefficients at the excitation wavelength.

The relaxation $A^* \rightarrow A$ should consist of the internal conversion in the dopant and the subsequent intermolecular vibrational energy transfer from the dopant to the surrounding matrix polymer. As a result, the matrix polymer should be heated up repeatedly during the multiphoton absorption. When the laser fluence is high enough, the matrix polymer should thermally decompose rapidly, resulting in ablation.[1–7] The expected temperature increase of the matrix polymer has been confirmed qualitatively on the basis of the broadening of the dopant fluorescence spectra.[5,6] However, there has been no quantitative discussion about the thermal dynamics of the matrix polymer including its rapid temperature increase, mainly because there has been much difficulty in the temperature measurement on a nanosecond time-scale. Dlott et al. has reported an approach to estimate the rapid temperature elevation of PMMA doped with IR-165 under picosecond or nanosecond laser excitation.[8–11] Unfortunately, their estimation technique can not applied to our present study for the following reasons: First, their excitation wavelength is 1064 nm, far from UV. Second, their temperature estimation is based on the specific temperature dependence of the photoabsorption by IR-165 at 532 or 633 nm.

The purpose of this work, therefore, is to investigate the thermal dynamics quantitatively by using an original method based on the diffusion of a dopant in the T_1 state. The main focus is to make use of the temperature-dependent T_1-T_1 annihilation. El-Sayed et al. indicated, after examining the phosphorescence decays of several aromatic molecules in PMMA, that a temperature increase from 77 K to about 300 K results in the appearance of effective T_1-T_1 annihilation due to increased diffusion of the solute aromatics.[13] They also indicated that the Arrhenius plots of the obtained second-order rate constants (k_2) for the annihilation are well fitted to straight lines. We applied their finding to the temperature estimation at higher temperatures. We used similar Arrhenius plots to estimate the k_2 values at high temperatures after intense laser excitation. We developed a computer simulation of the temperature change caused by laser excitation and the resulting temperature-dependent T_1 decay with the estimated k_2 values. The comparison of the T_1 decays observed by transient absorption spectroscopy with those calculated by the simulation revealed the thermal dynamics of the doped-polymer after intense laser excitation.

For the present purpose, the chosen dopants are biphenyl and *p*-terphenyl, mainly because the experimental data of both dopants has been well accumulated, including our previous ablation studies.[3,14–16]

Experimental

Samples. PMMA (polymerization degree ≈1000, supplied by Kuraray Co. Ltd.) was purified by reprecipitating it from benzene solution with methanol repeatedly. Biphenyl (zone refined, Tokyo Kasei) was used as received. *p*-Terphenyl (Scintillation grade, Tokyo Kasei) was purified by a homemade zone-refiner. Chlorobenzene (99%, Wako) was purified by shaking repeatedly with portions of sulfuric acid. It was then washed with water, followed by dilute sodium hydroxide solution, dried with anhydrous calcium chloride, and fractionally distilled. Sample films, biphenyl-doped PMMA (BP/PMMA) and *p*-terphenyl-doped PMMA (PT/PMMA), were prepared by spin-coating on a quartz plate from the solution of PMMA and dopant (biphenyl or *p*-terphenyl) in chlorobenzene. The films were dried under vacuum at room temperature for several hours. The dopant concentration and absorption coefficient of BP/PMMA were 0.093 M and 0.41 μm^{-1}, respectively, and those of PT/PMMA were 0.14 M and 0.26 μm^{-1}, respectively. The film thickness of both BP/PMMA and PT/PMMA was 2 μm, except that it was 1 μm for the T_1 absorption decay measurement under intense excitation.

Laser Irradiation. A KrF excimer laser (248 nm, Lambda Physik, EMG201MSC) was used for the irradiation of the films. The laser pulse width was about 30 ns. The laser pulse was trimmed through an aperture and focused normally (except for the temperature-controlled experiment described below) onto a film surface by using a quartz lens. The laser fluence was adjusted by placing partially transmitting laser mirrors in front of the laser output. In the case of intense excitation (a laser fluence higher than 10 mJ/cm^2), we irradiated a fresh film surface to avoid complexities arising from the interactions between the irradiated surface and the successive laser pulses. To monitor the laser absorption by the sample films, we observed the incident and transmitted excitation laser pulses with two photodiodes.

Transient Absorption Measurement at Various Temperatures. Figure 2 shows the experimental set-up for transient absorption measurement at controlled temperatures. The sample film was placed in a vacuum photolysis chamber equipped with quartz windows. The pressure inside the chamber was about 1 ×

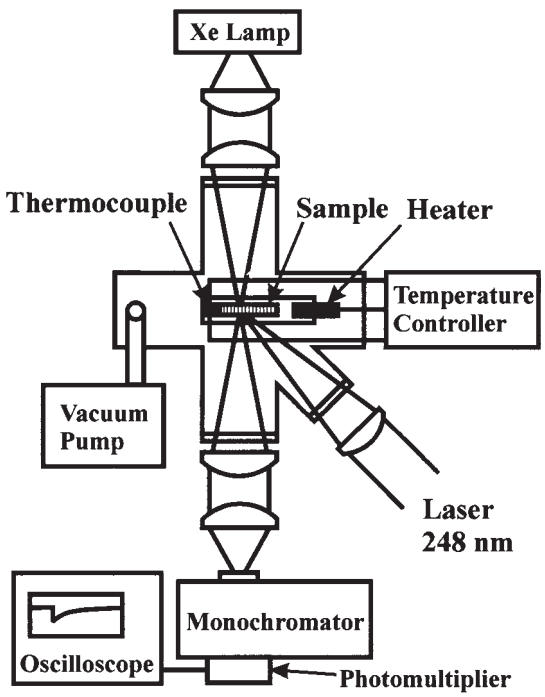

Fig. 2. Experimental set-up for transient absorption measurement at controlled temperatures.

10^{-3} Torr. The film was interposed between two copper plates attached to a ceramic heater. A thermocouple was also attached to the sample quartz plate. Both heater and thermocouple were electrically controlled by a temperature controller to achieve and keep a desired temperature (~363 K). The sample film was irradiated with a 2–4 mJ cm^{-2} pulse whose fluence was low enough to neglect the temperature elevation by laser excitation. A pulsed 150 W xenon lamp (Wakom, KXL-150F or Hamamatsu, L2274) was used as a monitoring light source. The monitoring light was incident vertically to the film while the excitation laser was incident at 45° to the film. The transmitted monitoring light was passed through a monochromator and detected by a photomultiplier (RCA, 1P28). The photocurrent signal ran into a 1–50 kΩ terminator and the resulting voltage signal was monitored and recorded on a digital oscilloscope (Hewlett-Packard, HP54510A). The transient absorption decay was calculated on a personal computer from the time profiles of the signals with and without excitation.

Transient Absorption Measurement under Intense Excitation. The details of the transient absorption measurement under intense excitation were described elsewhere,[4,16] and we only summarize them here. A pulsed 150 or 300 W xenon lamp (Wakom, KXL-150F or KXL300F) was used as a monitoring light source. The monitoring light was incident at 45° to the film, while the excitation laser was incident vertically to the film.[17] The transmitted monitoring light was detected and recorded by using a combination of a polychromator (Jovin Yvon, HR-320) and a streak camera system (Hamamatsu, C2830 and C3140). The streak images with and without laser excitation were averaged over more than 10 measurements, from which the rise-and-decay curves were obtained. The origin of the time axis, 0 ns, is defined as the time when the intensity of the excitation laser pulse at the film surface became maximum. The measurements were done in air at room temperature.

Results and Discussion

Confirmation of the Cyclic Multiphotonic Absorption. A preliminary experiment confirmed that the ablation thresholds of BP/PMMA and PT/PMMA are 330 mJ cm^{-2} and 280 mJ cm^{-2}, respectively. In the present study, we irradiated the sample films below the ablation thresholds to eliminate complexities arising from morphological changes, such as scattering of the monitoring lights. From the observation of the incident and transmitted excitation laser pulses, we calculated the effective absorbance at the excitation wavelength of 248 nm (Fig. 3a). With an increase in the excitation fluence, the absorbance of both films decreases up to about 100 mJ cm^{-2}, and then reaches almost steady values. This is undoubtedly because intense laser excitation produces appreciable amounts of transient states that have absorption coefficients different from that of the ground state. To specify the transient states contributing to the absorbance change is an interesting but quite difficult subject,[5] and here we only concentrate on the energy absorption and dissipation of the sample films.

From the effective absorbance, the dopant concentration, the film thickness, and the fluence, we can calculate the number of photons absorbed per dopant molecule averaged over the film (Fig. 3b). This calculation clearly shows that the numbers increase with an increase in the laser fluence, and that both dopants absorb several 248 nm photons slightly below the ablation thresholds. Figure 4 shows the absorption spectra of the sample films, which were measured on a conventional spectrophotometer, before and after laser irradiation (220 mJ cm^{-2} for BP/PMMA and 190 mJ cm^{-2} for PT/PMMA). The characteristics of the absorption spectra after the irradiation are the same for both samples. Namely, the spectra after the irradiation became slightly broader, and the absorbance around the peak slightly decreased, while the absorbance in the tails slightly increased. However, in spite of the characteristics of the changes mentioned here, we can safely conclude from Fig. 4 that almost all the dopants in PMMA survive after the intense irradiation. Note that about 10 photons are absorbed per dopant for BP/PMMA at 220 mJ cm^{-2} and that about 6 photons are absorbed per dopant for PT/PMMA at 190 mJ cm^{-2}. The survival of the dopants after the absorption of several UV photons indicates a quite efficient transfer of the absorbed photon energy from the dopants to the matrix polymer, which is in good agreement with the cyclic multiphotonic

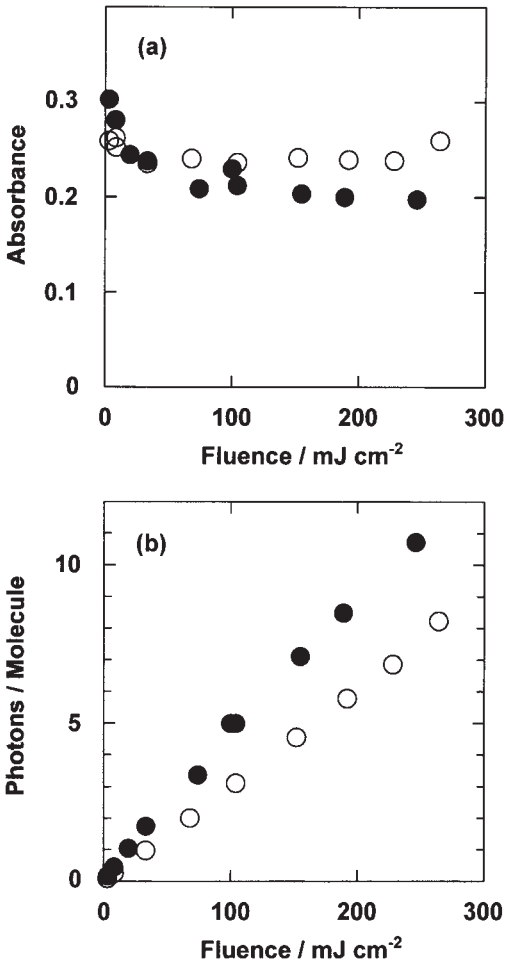

Fig. 3. Quantitative analysis of the fluence dependent photoabsorption by the sample films. (a) Fluence dependence of the effective absorbance at the excitation laser wavelength of 248 nm. (b) Fluence dependence of the absorbed photon number per dopant. Closed circles show the data for biphenyl-doped poly(methyl methacrylate), while open circles show those for *p*-terphenyl-doped poly(methyl methacrylate).

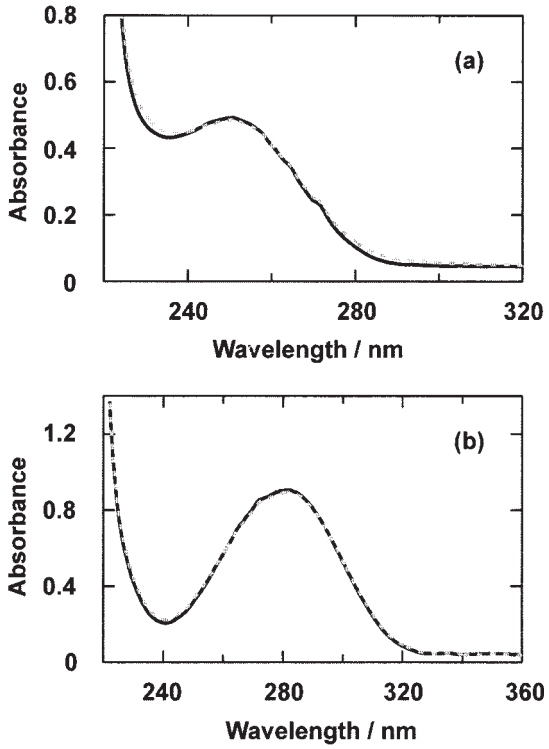

Fig. 4. Absorption spectral changes of poly(methyl methacrylate) doped with (a) biphenyl and with (b) *p*-terphenyl. The black solid and gray dashed lines represent the spectra before and after laser irradiation; the laser fluences were 220 mJ cm^{-2} for biphenyl-doped poly(methyl methacrylate) and 190 mJ cm^{-2} for *p*-terphenyl-doped poly(methyl methacrylate), respectively.

absorption mechanism.

Quite similar results regarding both multiphoton absorption and dopant survival have been reported for pyrene-doped PMMA previously.[5] Furthermore, experimental results of aromatic molecules in several organic solvents suggested that cyclic multiphotonic absorption also occurs in liquid matrices.[18–20] Therefore, our proposed mechanism should be generally true for light-absorbing molecules in condensed matrices under intense excitation. In addition to the pure photophysical interests described above, cyclic multiphotonic absorption has also become important in practical applications. Recent papers reported that cyclic multiphotonic absorption should occur in the following novel micro-fabrication processes: (i) laser molecular implantation into polymer films;[21–24] (ii) etching of fused silica in contact with acetone doped with pyrene.[19,20]

Temperature Dependence of T_1-T_1 Annihilation. We investigated the decay profiles of the $T_n \leftarrow T_1$ absorption for both BP/PMMA (370 nm) and PT/PMMA (455 nm) at every 10 K from 293 K (20 °C) to 363 K (90 °C); Figure 5 shows the decay profiles at 313 K and 353 K. For both films the decay became rapid with an increase in the temperature, which is well interpreted in terms of diffusion-controlled T_1-T_1 annihilation.[5,13] This annihilation occurs when a certain pair of T_1 states collides with each other through diffusion in a matrix polymer, and thus can be treated as a bimolecular reaction. The decay kinetics of the T_1 state are expressed by

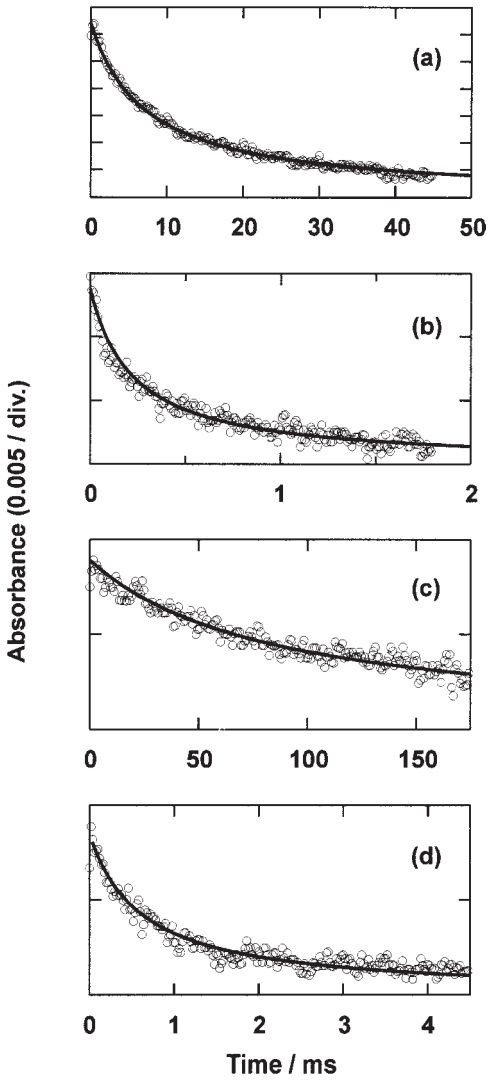

Fig. 5. Temperature dependence of the $T_n \leftarrow T_1$ absorption decay. Open circles show the decay of 370 nm absorption of biphenyl-doped poly(methyl methacrylate) at (a) 313 K and (b) 353 K and the decay of 455 nm absorption of *p*-terphenyl-doped poly(methyl methacrylate) at (c) 313 K and (d) 353 K. The solid lines show the least-squares fits to the circles based on the model of the second-order annihilation process described in the text.

$$\frac{d[T_1]}{dt} = -k_1[T_1] - k_2[T_1]^2 \quad (1)$$

where k_1 (s^{-1}) is a first-order rate constant and k_2 (M^{-1} s^{-1}) is a second-order rate constant corresponding to the T_1-T_1 annihilation. If $k_2[T_1] \gg k_1$, the right side of Eq. 1 can be simplified to $-k_2[T_1]^2$. In the present experiment, this simplified form is a good approximation even at room temperature; all the decay profiles were well analyzed only in terms of the T_1-T_1 annihilation. We integrated the simplified Eq. 1 and obtained:

$$A_{T_1,t} = \frac{1}{\frac{1}{A_{T_1,t=0}} + \frac{k_2}{\varepsilon_{T_1} d} t} \quad (2)$$

where $A_{T_1,t}$ is the absorbance observed at time t, ε_{T_1} is the molar absorption coefficient (27100 $M^{-1} cm^{-1}$ for biphenyl and 90000 $M^{-1} cm^{-1}$ for *p*-terphenyl),[25] and d is the film thickness in cm. We applied Eq. 2 to the least squares fitting of the decay profiles, and obtained the values of k_2 at every temperature for both BP/PMMA and PT/PMMA.

The diffusion of the T_1 state can occur two ways: The real diffusion of the dopants, and excitation transfer. In the present case, the only possible path of the latter is the $T_1 \rightarrow S_0$ excitation transfer, because no transient state other than the T_1 state was detected spectroscopically after the laser pulse. The $T_1 \rightarrow S_0$ excitation transfer occurs through the short range interaction of electron exchange.[26] Accordingly, its occurrence also needs the formation of an encounter pair of both states through diffusion. Furthermore, this excitation transfer only results in the exchange of both states in the pair. Therefore the $T_1 \rightarrow S_0$ excitation transfer has quite a minor effect on the diffusion of the T_1 state; in other words, T_1 diffusion occurs primarily by the molecular diffusion of the dopants. From this, the second-order rate constant k_2 can be related to the diffusion coefficient D ($cm^2 s^{-1}$) by

$$k_2 = 16 \times 10^{-10} \pi pRND \quad (3)$$

where N is Avogadro's number, R is the molecular radius in nm,[13] and p (≤ 2) is defined as the average number of the annihilated T_1 states in each collision. We assume here that the present annihilation is in the diffusion limit ($p = 2$); Fang et al. confirmed, in the case of benzophenone in benzene solution, that the second-order rate constant of T_1-T_1 annihilation is very near the diffusion limit.[27] At room temperature (293 K) Eq. 3, with the experimentally obtained values of k_2, gives the following values of the diffusion coefficients in PMMA, $D = 4 \times 10^{-13}$ $cm^2 s^{-1}$ for biphenyl and $D = 7 \times 10^{-13}$ $cm^2 s^{-1}$ for *p*-terphenyl; we assumed $R = 0.7$ nm for biphenyl and $R = 1.1$ nm for *p*-terphenyl on the basis of typical values of chemical bond lengths. The obtained values are the lowest limits using $p \leq 2$, and thus in good agreement with the previous suggestion of $D \approx 10^{-12}$ $cm^2 s^{-1}$ for several hydrocarbons (naphthalene, fluorene, perfluorobiphenyl, triphenylene, and coronene).[13]

The diffusion of aromatic molecules in a polymer should be a thermally activated process involving small-scale translational motions in the molecule or segment motion in the polymeric medium, and thus the diffusion coefficient can be expressed in Arrhenius form:

$$D = D_A \exp\left(-\frac{E_d}{RT}\right) \quad (4)$$

where D_A and E_d are the preexponential factor and the activation energy of diffusion, respectively.[28] On the basis of Eqs. 3 and 4, we made Arrhenius plots of k_2 (Fig. 6). Both plots were well fitted with straight lines, and then gave:

$$k_2 = 1.74 \times 10^{21} \exp(-1.22 \times 10^4/T) \quad \text{for BP/PMMA} \quad (5)$$

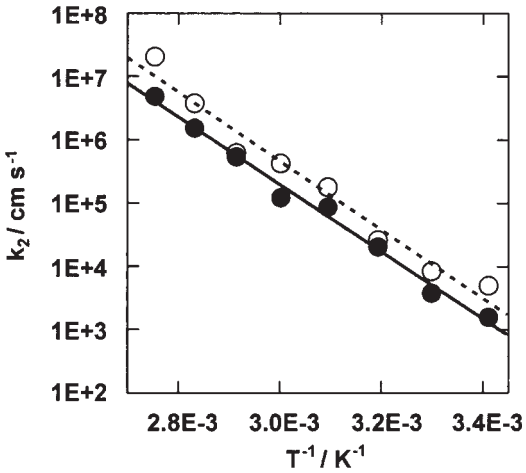

Fig. 6. Arrhenius plots of the second-order rate constant of the T_1 state for biphenyl-doped poly(methyl methacrylate) (closed circles) and *p*-terphenyl-doped poly(methyl methacrylate) (open circles). The solid and dashed lines are linear least-squares fits to the circles for biphenyl-doped poly(methyl methacrylate) and *p*-terphenyl-doped poly(methyl methacrylate), respectively.

$$k_2 = 9.11 \times 10^{21} \exp(-1.25 \times 10^4/T) \quad \text{for PT/PMMA} \quad (6)$$

where T is the film temperature. The activation energy was calculated to be 102 kJ mol^{-1} for BP/PMMA and 104 kJ mol^{-1} for PT/PMMA. These values are in good agreement with the previously reported values (ca. 50–100 kJ mol^{-1}) for the diffusion of the hydrocarbons mentioned above in PMMA at around room temperature.[13]

To simulate the T_1 absorption decay under intense excitation, we used Eqs. 5 and 6 to estimate the temperature dependent values of k_2. However, both equations are based on the decay analysis below the glass transition temperature, T_g, of PMMA (ca. 378 K),[29] and thus their validity above T_g should be discussed before any calculation. It is believed that the translational motion of small molecules in the polymer matrix is assisted by the formation of thermally activated packets of free volume.[28] In solid polymers above T_g, large-scale segmental motions occur and impart relatively large amounts of free volume. This may allow much more efficient diffusion above T_g with high activation energy of the segmental motions. In this case, the Arrhenius plot of the diffusion coefficient strongly changes its slope above T_g and accordingly the use of Eqs. 5 and 6 above T_g is quite inappropriate. On the basis of the experiments involving laser molecular implantation, however, the activation energy for the diffusion of anthracene in PMMA in the temperature range of ca. 500–800 K, well above T_g, was estimated to be 71 ± 10 kJ mol^{-1}.[21,22] This value is similar to those obtained for biphenyl and *p*-terphenyl below T_g in the present study. This result for anthracene, whose size is similar to that of the dopants used here, indicates that the application of Eqs. 5 and 6 above T_g is a good approximation.

This conclusion is well supported by the results of laser-induced holographic grating relaxation experiments.[30,31] Wang et al. applied this technique to the study of the diffusion of thy-

moquinone in poly(α-methyl styrene) and diacetyl in PMMA, and found the following points: (1) at the low dopant concentration limit, the diffusion coefficient rapidly decreases as the temperature is decreased below T_g, and the activation energy of the diffusion coefficient above T_g is much higher than that below T_g; (2) at higher dopant concentrations, the diffusion coefficient shows Arrhenius temperature dependence with no obvious change in the activation energy as T_g is traversed. The former case 1 corresponds to typical temperature dependence in the solid polymers described above. On the other hand, the latter case 2 is better explained by the plasticizing effect of a dopant.[31] Plasticizers induce the mobility of the polymer chains, hence increasing the local free volume fluctuation, which results in a higher diffusion coefficient. With the increase in local free volume, the chain motion somewhat loses its cooperativity as the glass transition temperature is approached. Thus, the diffusion coefficient is not expected to experience strong temperature dependence in the vicinity of T_g. In the present work, the similarity of the activation energy above and below T_g suggests that case 2 holds. This is supported by further analysis of the experimental results by Wang et al. In the case of 0.9 wt% diacetyl in PMMA, a temperature decrease of about 10 °C from 117 to 107.7 °C ($T_g = 115$ °C) resulted in a diffusion coefficient decrease of more than 3 orders of magnitude from 8.5×10^{-11} to 3.43×10^{-14} cm^2 s^{-1}.[29] Below 107.7 °C, the diffusion coefficient changed slowly with temperature. If this temperature dependence, clearly similar to case 1, applied to the present work, the diffusion coefficients of both biphenyl and *p*-terphenyl at room temperature should be on the order of, or smaller than, 10^{-14} cm^2 s^{-1} when we consider the sizes of the three dopants. The estimated values of $D \approx 10^{-12}$ cm^2 s^{-1} for both dopants, much higher than 10^{-14} cm^2 s^{-1}, should be the result of an increase in the local free volume fluctuation as a result of the plasticizing effect. Therefore, case 2 applies to both biphenyl and *p*-terphenyl in PMMA in the present experimental conditions, which ensures the application of Eqs. 5 and 6 above T_g.

Simulation of the Temperature and T_1 Decay. On the basis of the results described above, we made a computer simulation describing the temperature change caused by the laser excitation and the resulting temperature-dependent T_1 decay.

(i) General Features of the Simulation: The system in the simulation has three components of the air (85 μm in thickness), PMMA with biphenyl or *p*-terphenyl (1 μm in thickness), and quartz (15 μm in thickness), from left to right, in this order. These components are split into 190 (air), 60 (PMMA), and 200 (quartz) thin layers, numbered from 1 (left-hand side of the air) to 450 (right-hand side of the quartz), as a control layer for the simulation of the following three phenomena: absorption of photon energy by the doped-polymer; temperature change by the thermal conduction through the air, polymer, and quartz; temperature-dependent T_1-T_1 annihilation. To simplify the calculation, we only consider one dimensional heat flow along the axis (*x* axis) vertical to both air-polymer and polymer-quartz interfaces. This treatment is a good approximation in the present case, where the purpose of the simulation is to compare calculated results with the experimentally observed T_1 decays. In particular, we paid special attention to keep the experimental condition that the irradiation area of the monitoring light is smaller than, and within that, of the excitation laser pulse. Therefore, the monitored region may be regarded as being surrounded by a bath of similar temperature, and the lateral thermal diffusion may safely be neglected.

The cross section of each control layer is set to be 1 cm^2 for the convenience of the calculation. The simulation contains only one parameter, r ($0 \sim 1$), the ratio of the energy used to increase the polymer temperature to the photon energy absorbed by the polymer. For example, $r = 1$ means that all the absorbed energy is used to increase the temperature. By changing the value of r in the simulation, we found the most plausible value that gives the best reproduction of the observed T_1 absorption decay.

(ii) Absorption of Photon Energy: On the basis of the monitoring of the photoabsorption by the sample films (Fig. 3), we obtained empirical equations of the irradiated fluence F (J cm^{-2}) and absorbed fluence AF (J cm^{-2}) as follows:

$$AF = 0.607 + 0.390F - 1.49 \times 10^{-4}F^2 \quad \text{for BP/PMMA} \quad (7)$$

$$AF = 0.391 + 0.389F + 1.41 \times 10^{-4}F^2 \quad \text{for PT/PMMA} \quad (8)$$

The laser pulse, whose time profile was obtained experimentally, as shown in Figs. 7 and 8, is split into a sequential pulse train of short rectangular pulses whose pulse width is 0.03 ns. This pulse width is used as the time step of the simulation (Δt). For each arrival and passage of a rectangular pulse, the distribution of the absorbed energy among the 60 thin layers of the polymer is calculated on the assumption that each layer has the same absorption coefficient α (cm^{-1}) expressed by

$$\alpha = \ln\{F/(F - AF)\}/d \quad (9)$$

This assumption is appropriate in the present case because, as mentioned later, our simulation was done only for fluences in the range of 100–190 mJ cm^{-2} where the effective absorbance gives steady values, as shown in Fig. 3a.

(iii) Temperature Change: The initial temperature of each control layer is set to room temperature, 293 K. The simulation of the thermal conduction is based on Fourier's law:

$$q = -\lambda \frac{\partial T}{\partial x} \quad (10)$$

where q is the heat flux in the x direction and λ is the thermal conductivity of the material through which the heat flows. By applying a finite difference scheme to Eq. 10, the heat flux from $i-1$ th to ith control layer, $q_{i,i-1}$ (W cm^{-2}), can be written as:

$$q_{i,i-1} = -\frac{T_i - T_{i-1}}{(d_i/2)/\lambda_i + (d_{i-1}/2)/\lambda_{i-1}} \quad (11)$$

where T_i (K), d_i (cm), and λ_i (W cm^{-1} K^{-1}) denote the temperature, thickness, and thermal conductivity of the ith layer at time t, respectively.[32] Note that Eq. 11 can calculate the heat flux between the control layers with different thermal conductivities. This is quite important in this simulation, be-

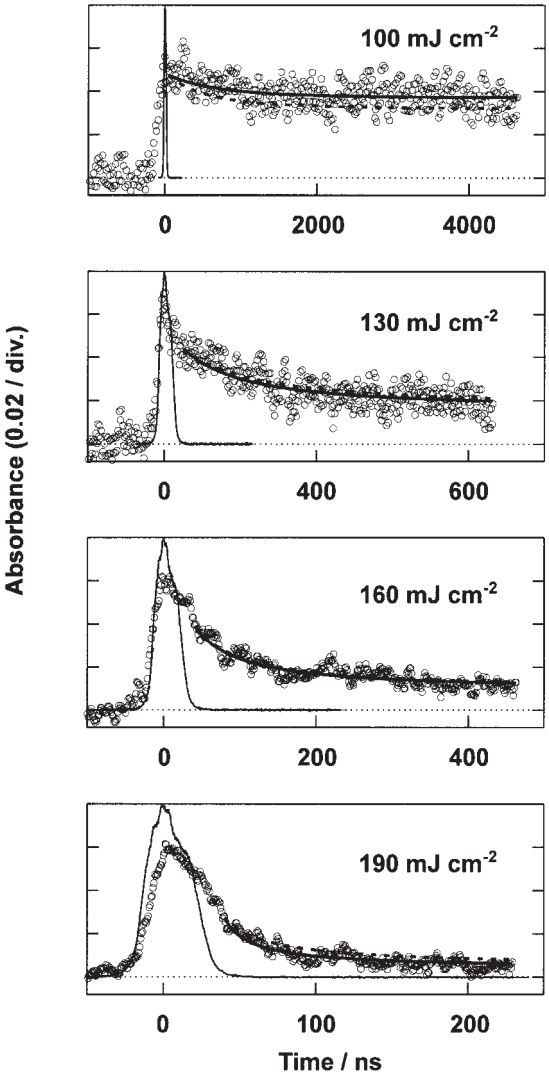

Fig. 7. Fluence dependence of the rise-and-decay profiles of the absorption at 370 nm of biphenyl-doped poly(methyl methacrylate). The open circles show the experimentally obtained profiles and the thin solid lines show the time profiles of the laser pulse. The thick lines show the simulated decay profiles based on the temperature-dependent second-order annihilation process and the cooling process of the matrix polymer where the parameter r is the ratio of the energy used to increase the polymer temperature to the photon energy absorbed by the polymer: the thick solid lines show the best-fits to the experimental profiles at 100 mJ cm^{-2} ($r = 0.73$), 130 mJ cm^{-2} ($r = 0.83$), 160 mJ cm^{-2} ($r = 0.82$), and 190 mJ cm^{-2} ($r = 0.87$); the thick dashed lines show the simulated profiles with the mean value of $r = 0.81$.

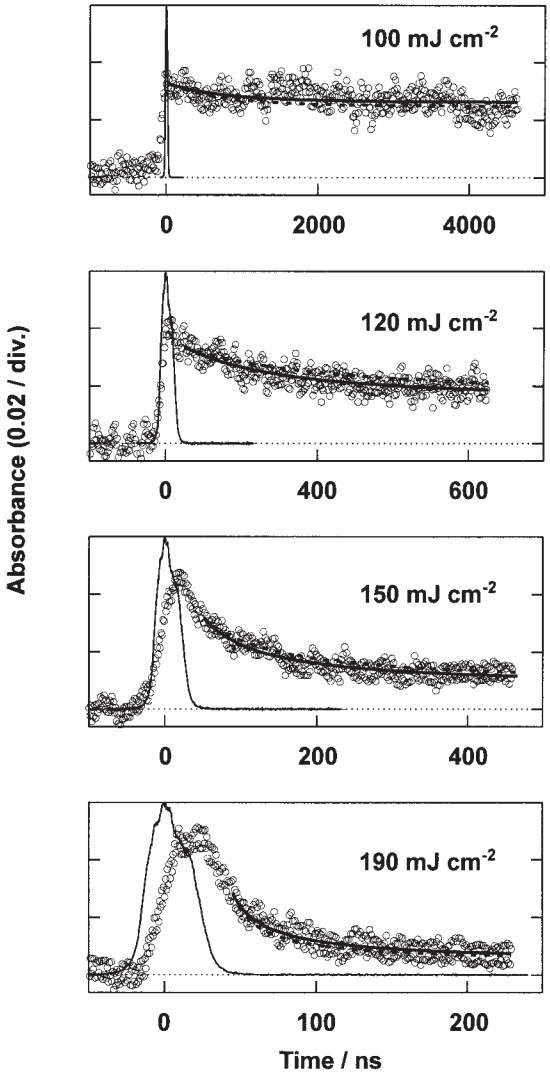

Fig. 8. Fluence dependence of the rise-and-decay profiles of the absorption at 455 nm of *p*-terphenyl-doped poly(methyl methacrylate). The open circles show the experimentally obtained profiles and the thin solid lines show the time profiles of the laser pulse. The thick lines show the simulated decay profiles based on the temperature-dependent second-order annihilation process and the cooling process of the matrix polymer where the parameter r is the ratio of the energy used to increase the polymer temperature to the photon energy absorbed by the polymer: the thick solid lines show the best-fits to the experimental profiles at 100 mJ cm^{-2} ($r = 0.83$), 120 mJ cm^{-2} ($r = 0.92$), 150 mJ cm^{-2} ($r = 0.90$), and 190 mJ cm^{-2} ($r = 0.84$); the thick dashed lines show the simulated profiles with the mean value of $r = 0.87$.

cause (i) there are two interfaces between the different materials (air-polymer and polymer-quartz) where a difference in the thermal conductivity apparently exists, and (ii) thermal conductivity depends on the temperature, and each layer has a different temperature. The temperature change (ΔT_i) of the ith control layer after a time step Δt is expressed by:

$$\Delta T_i = \{(q_{i,i-1} - q_{i+1,i})\Delta t + rE_i\}/(\rho_i C_i d_i) \quad (12)$$

where ρ_i (g cm^{-3}) and C_i (J g^{-1} K^{-1}) are the density and heat capacity of the ith control layer, respectively, and E_i is the photon energy absorbed by the ith control layer. The term rE_i represents the amount of energy that contributes to the temperature increase. It is apparent from the definition of E_i that E_i becomes zero after the laser pulse, and thus the term rE_i, as well as the parameter r, are valid only within the laser pulse. As the boundary condition, we adopted the adiabatic approxi-

mation of $q_{0,1} = q_{450,451} = 0$, and accordingly set the widths of the air and quartz (85 and 15 μm) large enough to neglect the thermal diffusion at the air and quartz ends. After the simulation, we took care to confirm that the temperatures of both layers 1 and 450 remained unchanged.

In the simulation of the temperature change, as shown in Eqs. 11 and 12, we need the values of the density (ρ_{air}, ρ_{PMMA}, ρ_{quartz}), heat capacity (C_{air}, C_{PMMA}, C_{quartz}), and thermal conductivity (λ_{air}, λ_{PMMA}, λ_{quartz}). We consulted Ref. 29 for PMMA and Ref. 33 for air and quartz. In case there existed values at several appropriate temperatures between 293 and 600 K, we made empirical equations for the physical constants that reproduce the temperature dependence. Otherwise, we adopted the values at certain temperatures. Finally, for density, we used the following values: $\rho_{air} = 1.161 \times 10^{-3}$ g cm^{-3} (at 300 K), $\rho_{PMMA} = 1.188$ g cm^{-3} (at 298 K), and $\rho_{quartz} = 2.2$ g cm^{-3}.[34] For heat capacity, we used $C_{air} = 1.0$ J g^{-1} K^{-1} (at 300 K) and the following equations:

$$C_{PMMA} = -1.78 + 0.0142T - 1.18 \times 10^{-5}T^2 \quad \text{J g}^{-1}\,\text{K}^{-1} \tag{13}$$

$$C_{quartz} = 0.0407 + 0.00295T - 2.07 \times 10^{-6}T^2 \quad \text{J g}^{-1}\,\text{K}^{-1} \tag{14}$$

For thermal conductivity, we used $\lambda_{PMMA} = 1.9 \times 10^{-3}$ W cm^{-1} K^{-1} (273–323 K) and the following equations:

$$\lambda_{air} = 1 \times 10^{-5} + 9.79 \times 10^{-7}T - 3.68 \times 10^{-10}T^2 \quad \text{W cm}^{-1}\,\text{K}^{-1} \tag{15}$$

$$\lambda_{quartz} = 4.96 \times 10^{-3} + 4.25 \times 10^{-5}T - 3.45 \times 10^{-8}T^2 \quad \text{W cm}^{-1}\,\text{K}^{-1} \tag{16}$$

(iv) T_1-T_1 Annihilation: The T_1 absorption of a certain doped-polymer control layer, ($A_{T_1,i}$), is calculated according to the following finite difference equation:

$$\Delta A_{T_1,i} = -\frac{k_2}{\varepsilon_{T_1} d_i} A_{T_1,i}{}^2 \Delta t \tag{17}$$

which is based on Eq. 1 with the approximation of $k_1[T_1] = 0$. The summation of $A_{T_1,i}$ over the 60 layers gives A_{T_1}, which is the T_1 absorption of the whole film.[35] The constant k_2 is temperature dependent and calculated by Eq. 5 (BP/PMMA) or 6 (PT/PMMA). During laser excitation, there are many complicated processes, such as photoabsorption by the T_1 state, and thus the starting point of the absorption simulation is set to be just after the laser pulse. The initial value of A_{T_1} of the simulation is determined from the experimental data, and then the initial value of each $A_{T_1,i}$ is determined according to the distribution of the absorbed photon energy. We assumed that the T_1 concentration in a certain layer is proportional to the energy absorbed by the layer.

Decay Dynamics of the T_1 States under Intense Excitation. Open circles in Figs. 7 and 8 show the fluence dependence of the absorption decay of the T_1 state for BP/PMMA and PT/PMMA respectively. For both films, the decay became rapid with an increase in the laser fluence. This characteristic fluence dependence has already been reported for pyrene-,[5] TMPD-,[7] *p*-terphenyl-,[14,15] biphenyl-doped PMMA,[16] and is ascribed to the thermally facilitated T_1-T_1 annihilation. As mentioned previously, repetitive simulations changing the value of the parameter *r* gave best fits (solid lines in Figs. 7 and 8) to the experimentally obtained T_1 decay profiles at 100–190 mJ cm^{-2}, where the decay dynamics dramatically change with an increase in the fluence. Note that above 190 mJ cm^{-2} the T_1 absorption decays out within the laser pulse and thus the fitting by the simulation is invalid. The values of *r* range from 0.73 to 0.87 for BP/PMMA and from 0.83 to 0.92 for PT/PMMA. For reference, the simulation results with the mean value of *r* (0.81 for BP/PMMA and 0.87 for PT/PMMA) are also shown in Figs. 7 and 8 as dashed lines. At present, we can hardly conclude whether the observed slight scatter of *r* arises from some substantial photophysics or just an experimental error. We can safely conclude, however, that most of the absorbed photon energy, at least 70% of it, is used to increase the temperature of the polymer. This conclusion supports the viewpoint that aromatic molecules in a polymer can work as a good "molecular heater" under intense laser excitation.[8–11]

The high conversion efficiency shown by both dopants is quite interesting when we consider their conventional fluorescence quantum yields (0.15 for biphenyl and 0.77 for *p*-terphenyl).[25] It suggests that intense excitation opens novel radiationless pathways which are common for aromatic molecules and independent of conventional radiative pathways. Actually, a similar suggestion based on the fluorescence decay of anthracenes gave rise to the assertion of the cyclic multiphotonic absorption mechanism, where cyclic photoabsorption ($A \rightarrow A^* \rightarrow A$) corresponds to such a pathway.[2]

The cyclic photoabsorption mechanism also explains the efficient conversion of the absorbed photon energy into thermal energy. We have to consider, however, another process in the excited state interactions because of the high dopant concentrations (≈0.1 M) chosen here. Actually, we have experimentally confirmed the substantial production of both S_1 and T_1 states within the laser pulse for both BP/PMMA and PT/PMMA.[15,16] Therefore, excited state interactions, such as S_1-S_1 and T_1-T_1 annihilation, should occur during the laser excitation. This should result in the efficient deactivation of the electronic excitation energy, and thus also contribute to the energy conversion. At the present stage, both mechanisms seem quite possible and there is little information about the extent of the contribution of each mechanism. To obtain such information, a reduction of the dopant concentration should be informative because the cyclic multiphotonic absorption may apply to the diluted condition in contrast to the excited state interactions, which require a high concentration.

With respect to the energy dissipation pathways, other than thermal ones, we can make some qualitative discussions. One definite pathway is the $S_1 \rightarrow S_0$ radiative transition (fluorescence) of the dopant, which was experimentally detected for both films.[15,16] Another possible pathway is the thermally induced bond breaking of the polymer. Previous experiments have confirmed that degradation of a polymer occurs to some extent even below the ablation threshold.[4,36]

Not only does the temperature increase via laser excitation affect the dynamics of the T_1 state but also the cooling of

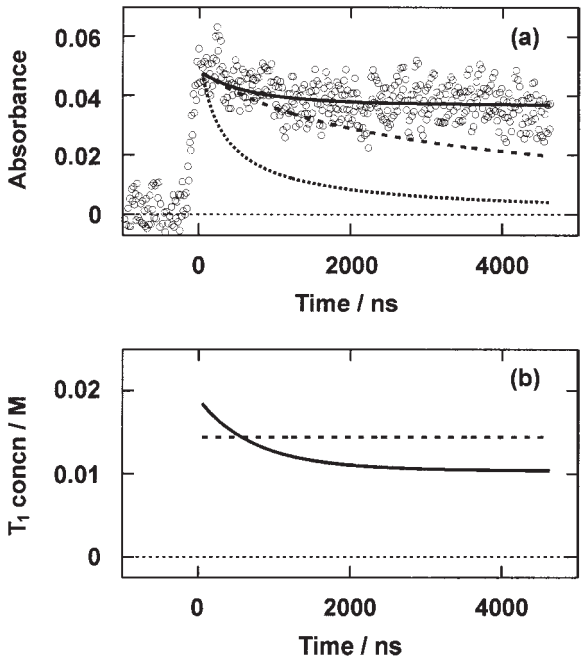

Fig. 9. Influence of the heat transfer to the quartz plate on the T_1 state dynamics of biphenyl-doped poly(methyl methacrylate) at 100 mJ cm^{-2} excitation. (a) The open circles show the experimentally obtained absorption rise-and-decay profile at 370 nm, while the solid line shows the simulated decay profile with $r = 0.73$; they are the same as those shown in Fig. 7. The dashed and dotted lines show the simulated profiles in the case of no thermal conduction with $r = 0.73$ and $r = 1$, respectively. (b) The comparison of the decays of the T_1 state simulated at the surface (solid line) and bottom (dashed line) of the film; the simulation condition is the same as that for the solid line ($r = 0.73$) in (a).

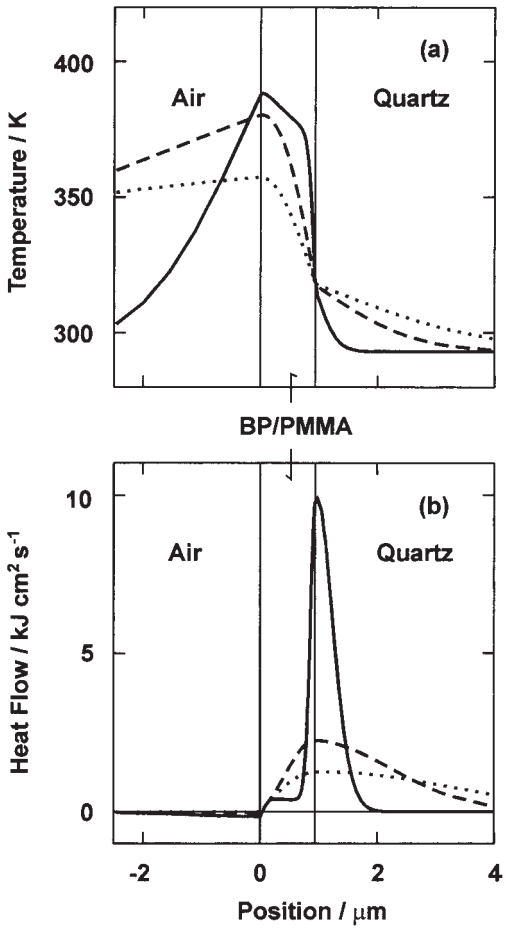

Fig. 10. Thermal dynamics of the air, biphenyl-doped poly(methyl methacrylate), and quartz at 100 mJ cm^{-2} excitation; all the shown profiles are derived from the best fit ($r = 0.73$) to the observed T_1 decay (100 mJ cm^{-2}) in Fig. 7. The position of the air-polymer interface is defined as 0 μm. (a) The solid, dashed, and dotted lines show the transient temperature distributions at 50 ns, 1 μs, and 3 μs respectively. (b) The solid, dashed, and dotted lines show the heat flow distributions at 50 ns, 1 μs, and 3 μs respectively; positive values refer to the heat flow from left to right.

the polymer, a typical example of which is shown in Fig. 9 for BP/PMMA at 100 mJ cm^{-2}. Note that the open circles and solid line in Fig. 9a are the same as those in Fig. 7. In Fig. 9a, the simulated absorption decay profile in the case of no thermal conduction with $r = 1$ (the dotted line) is totally different from the experimentally obtained one. The change of the parameter value to $r = 0.73$ gave a profile (the dashed line) still different from the experimental one. The simulation can reproduce the decay profile (the solid line) only with the additional consideration of thermal conduction. We confirmed that only changing the value of r does not give a good reproduction of the profile. Thus, the difference between the solid and dashed lines in Fig. 9a shows the influence of the thermal conduction on the T_1 decay. The cooling of the polymer film slows down the diffusion of the dopant, and, accordingly, the T_1-T_1 annihilation. Another result of the cooling effect is shown in Fig. 9b. At the surface of BP/PMMA (air side) the T_1 state decays, apparently by annihilation, but shows no decay at the bottom (quartz side) due to the efficient cooling by the heat transfer to the quartz. This will be discussed in the next subsection. It is necessary to consider the heat transfer to the substrate for discussions about laser heating effects in doped polymers including the T_1 state dynamics.

Thermal Dynamics of the Doped-polymer Film. The simulation with the determined value of r reveals additional detail about the thermal dynamics in the polymer, a typical example of which is shown in Fig. 10. This is the case of BP/PMMA at 100 mJ cm^{-2}, but quite similar characteristics are observed with different fluences and the other sample, PT/PMMA. At 50 ns, immediately after the excitation laser pulse, heat transfer from PMMA to both air and quartz is obvious from the temperature increase and distribution in both materials (Fig. 10a). There exists, however, different characteristics in the temperatures at the air-polymer interface ($T_{A\text{-}P}$) and polymer-quartz interface ($T_{P\text{-}Q}$). The value of $T_{A\text{-}P} = 388$ K is close to that expected in the case of no thermal conduction (390 K), while the value of $T_{P\text{-}Q} = 320$ K is well below that expected in the case of no thermal conduction (372 K). Furthermore, the time-dependent changes of $T_{A\text{-}P}$ and $T_{P\text{-}Q}$

Table 1. Comparison of the Thermal Properties of Air, Poly(methyl methacrylate) (PMMA), and Quartz[a)]

Material	ρC/J cm^{-3} K^{-1}	$a\left(=\frac{\lambda}{\rho C}\right)$/cm^2 s^{-1}	$b(=\sqrt{\lambda\rho C})$/J s$^{-1/2}$ cm^{-2} K^{-1}
Air	1.2×10^{-3}	2.5×10^{-1}	5.8×10^{-4}
PMMA	1.9	1.0×10^{-3}	5.9×10^{-2}
Quartz	1.7	8.6×10^{-3}	1.6×10^{-1}

a) Estimated at 320 K.

are also different from each other. $T_{A\text{-}P}$ gradually decreases to 357 K (3 μs), while $T_{P\text{-}Q}$ remains almost constant at ca. 320 K (319 K at 3 μs).

These characteristic differences are understood by the thermal conduction theory of the sudden contact of two solids at different temperatures.[37] In the present case, instead of sudden contact, it is nanosecond laser excitation that suddenly increases the temperature of the polymer between the air and quartz. According to the theory, when two solids (1 and 2) at different temperatures, T_1 and T_2, are brought into contact, the temperature at the point of contact changes instantly to T_0 and remains at this temperature for some time. The constant temperature T_0 is calculated as:

$$T_0 = \frac{b_1 T_1 + b_2 T_2}{b_1 + b_2} \tag{18}$$

where b_1 and b_2 are effusivities of solids 1 and 2, respectively. The effusivity b, defined as $b = (\lambda\rho C)^{-1/2}$, physically represents the capacity of a material to 'resist' an abrupt change in the temperature of its surroundings. A significant result of Eq. 18 is that the solid with the higher effusivity tends to impose its temperature, which is the case of $T_{A\text{-}P}$ at 50 ns ($b_{PMMA} \gg b_{air}$, see Table 1). Eq. 18 gives $T_0 \approx T_2$, if $b_2 \gg b_1$. On the other hand, the substitution of b_{PMMA}, b_{quartz} (Table 1), 372 K, and 293 K for b_1, b_2, T_1, and T_2 in Eq. 18 gives $T_{P\text{-}Q}\,(= T_0) = 314$ K which is in good agreement with that at 50 ns of the simulation.

The temperature changes in the later time region (~3 μs) are well understood with Fig. 10b of the heat flow distribution in the system. At 50 ns, in the air and the very thin surface layer of the polymer (up to 0.05 μm), the heat flows from right to left and its amount is quite small compared with that of the flow in the opposite direction at the interface of the polymer and the quartz. The ratio of the amount of the latter heat flow increases with time. Therefore, the temperature decrease of the polymer is mainly due to the heat transfer into the quartz plate. For example, we can easily calculate the total amount of the energy flowing out from the polymer to the air ($E_{P\to A}$) and that to the quartz ($E_{P\to Q}$); the ratio $E_{P\to Q}/E_{P\to A}$ is 86 at 3 μs. In spite of this ratio, the temperature of the air is much higher than that of the quartz, because air has a very small value of ρC (see Table 1). On the contrary, air has a large thermal diffusivity, $a = \lambda/(\rho C)$, compared with PMMA and quartz (see Table 1). This results in the relatively rapid disappearance of the temperature gradient in the air. The remaining interesting topic here is the constant temperature at the polymer-quartz interface. As can be seen in Fig. 10b, the heat flow has its maximum value in the vicinity of the polymer-quartz interface up to 3 μs. This results in a nearly zero divergence of the heat flow at the interface, which provides the physical background of the constant temperature. The peak position of the heat flow starts to leave the interface at about 3 μs and then gradually moves to the right, deeper inside the quartz (not shown in a Figure). As a result, the temperature $T_{P\text{-}Q}$ is no longer constant, and gradually decreases. The quasi-constant temperature discussed here may be useful for some future industrial application of laser heating of materials in contact with substrates.[19–24]

From the simulation, we can also obtain the fluence dependence of the maximum temperature (T_M) at the polymer surface (air side) reached by laser heating. With the mean values of r (0.81 for BP/PMMA and 0.87 for PT/PMMA), the temperature is estimated as follows: 400 K (100 mJ cm^{-2}), 420 K (130 mJ cm^{-2}), 440 K (160 mJ cm^{-2}), and 460 K (190 mJ cm^{-2}) for BP/PMMA; 400 K (100 mJ cm^{-2}), 420 K (120 mJ cm^{-2}), 440 K (150 mJ cm^{-2}), and 480 K (190 mJ cm^{-2}) for PT/PMMA. T_M increases with an increase in the fluence for both films, which reflects the efficient photoabsorption despite the intense excitation. These data are well fitted with straight lines, which corresponds to the fact that the effective absorbance is almost constant for both films in this fluence region (100–190 mJ cm^{-2}) as shown in Fig. 3a. Both lines are expressed by the following equations.

$$T_M = 0.67F + 330 \quad \text{for BP/PMMA} \tag{19}$$

$$T_M = 0.87F + 310 \quad \text{for PT/PMMA} \tag{20}$$

The intercepts of both lines, 330 K and 310 K, are higher than room temperature (293 K). This can also be explained by the fluence dependence of the absorbance shown in Fig. 3a. The absorbance in the low fluence region (<100 mJ cm^{-2}) is higher than the quasi-constant absorbance corresponding to the slopes of both lines. Therefore, T_M increases more rapidly in the low fluence region, which is the reason for the disparity. On the other hand, if we assume Eqs. 19 and 20 are valid in the higher fluence region (>190 mJ cm^{-2}), we can estimate the maximum temperature at the ablation threshold to be 550 K for both BP/PMMA (330 mJ cm^{-2}) and PT/PMMA (280 mJ cm^{-2}). The estimated value is in good agreement with that (530 K) of pyrene-doped PMMA at the ablation threshold.[5] It supports a reasonable hypothesis that there exists a specific temperature at which rapid thermal degradation of a polymer occurs leading to ablation.[38–40]

H. F. acknowledges the financial support of a Hiroshima City University Grant for Special Academic Research (General Studies) and of a Grant-in-Aid for Encouragement of Young Scientists (No. 09740440) from the Ministry of Education,

Science, Sports and Culture. We are grateful both to ANELVA Corp. for the use of the excimer laser and to Dr. M. Takagi of the Institute of Laser Engineering in Osaka University for the use of the depth profiler.

References

1 H. Fukumura, N. Mibuka, S. Eura, H. Masuhara, and N. Nishi, *J. Phys. Chem.*, **97**, 13761 (1993).

2 H. Fukumura and H. Masuhara, *Chem. Phys. Lett.*, **221**, 373 (1994).

3 H. Fujiwara, T. Hayashi, H. Fukumura, and H. Masuhara, *Appl. Phys. Lett.*, **64**, 2451 (1994).

4 H. Fujiwara, Y. Nakajima, H. Fukumura, and H. Masuhara, *J. Phys. Chem.*, **99**, 11481 (1995).

5 H. Fujiwara, H. Fukumura, and H. Masuhara, *J. Phys. Chem.*, **99**, 11844 (1995).

6 H. Fukumura, N. Mibuka, H. Fukumoto, and H. Masuhara, ''Laser Interaction and Related Plasma Phenomena,'' ed by S. Nakai and G. H. Miley, American Institute of Physics, New York (1996), pp. 1250–1255.

7 H. Fujiwara, H. Fukumoto, H. Fukumura, and H. Masuhara, *Res. Chem. Intermed.*, **24**, 879 (1998).

8 X. Wen, W. A. Tolbert, and D. D. Dlott, *Chem. Phys. Lett.*, **192**, 315 (1992).

9 I.-Y. S. Lee, X. Wen, W. A. Tolbert, D. D. Dlott, M. Doxtader, and D. R. Arnold, *J. Appl. Phys.*, **72**, 2440 (1992).

10 S. Chen, I.-Y. S. Lee, W. A. Tolbert, X. Wen, and D. D. Dlott, *J. Phys. Chem.*, **96**, 7178 (1992).

11 X. Wen, W. A. Tolbert, and D. D. Dlott, *J. Chem. Phys.*, **99**, 4140 (1993).

12 G. R. Fleming, ''Chemical Applications of Ultrafast Spectroscopy,'' Oxford University Press, New York (1986).

13 F. E. El-Sayed, J. R. MacCallum, P. J. Pomery, and T. M. Shepherd, *J. Chem. Soc., Faraday Trans. 2*, **75**, 79 (1979).

14 H. Masuhara and H. Fukumura, *Polym. News*, **17**, 5 (1991).

15 H. Fukumura, H. Hamano, and H. Masuhara, *Chem. Lett.*, **1993**, 245.

16 H. Fukumura, E. Takahashi, and H. Masuhara, *J. Phys. Chem.*, **99**, 750 (1995).

17 These incident angles were contrary to those of the transient absorption measurement at controlled temperatures. However the difference has no substantial meaning. It simply arises from an experimental restriction; the cell shown in Fig. 2 was originally designed for other experiments.

18 Y. Tsuboi, H. Fukumura, and H. Masuhara, *J. Phys. Chem.*, **100**, 10305 (1995).

19 J. Wang, A. Niino, and A. Yabe, *Appl. Phys. A*, **68**, 111 (1999).

20 J. Wang, A. Niino, and A. Yabe, *Appl. Phys. A*, **69**, S271 (1999).

21 H. Fukumura, Y. Kohji, K. Nagasawa, and H. Masuhara, *J. Am. Chem. Soc.*, **116**, 10304 (1994).

22 G. Gery, H. Fukumura, and H. Masuhara, *J. Phys. Chem. B*, **101**, 3698 (1997).

23 H. Fukumura, *J. Photochem. Photobiol., A*, **106**, 3 (1997).

24 H. Fukumura, H. Uji-I, H. Banjo, H. Masuhara, D. M. Karnakis, N. Ichinose, S. Kawanishi, K. Uchida, and M. Irie, *Appl. Surf. Sci.*, **127–129**, 761 (1998).

25 S. L. Murov, I. Carmichael, and G. L. Hug, ''Handbook of Photochemistry, 2nd ed,'' Marcel Dekker, New York (1993).

26 M. Koizumi, S. Kato, N. Mataga, T. Matsuura, and Y. Usui, ''Photosensitized Reactions,'' Kagakudojin Publishing, Kyoto (1978).

27 T.-S. Fang, R. Fukuda, R. E. Brown, and L. A. Singer, *J. Phys. Chem.*, **82**, 246 (1978).

28 J. Guillet, ''Advances in Photochemistry Vol. 14,'' ed by D. Volman, G. S. Hammond, and K. Gollnick, John Wiley & Sons, New York (1988).

29 J. Brandrup and E. H. Immergut, ''Polymer Handbook, 3rd ed,'' John Wiley & Sons, New York (1989).

30 J. Zhang and C. H. Wang, *Macromolecules*, **20**, 683 (1987).

31 C. H. Wang and J. L. Xia, *J. Chem. Phys.*, **92**, 2603 (1990).

32 S. V. Patankar, ''Numerical Heat Transfer and Fluid Flow,'' MacGraw-Hill, New York (1980).

33 ''CRC Handbook of Chemistry and Physics, 76th ed,'' ed by D. R. Lide and H. P. R. Frederikse, CRC Press, Boca Raton (1995).

34 There is no description of the temperature about the value of ρ_{quartz} that is based on information contained in Fused Quartz Catalogue Q-7A General Electric Company.

35 The path length of the monitoring light is 1.14 times as long as the film thickness d because of the refraction; we used the relationship of $60d_i = 1.14d$ in the simulation of T_1 absorption.

36 R. Srinivasan, B. Braren, and K. G. Casey, *J. Appl. Phys.*, **68**, 1842 (1990).

37 J. Taine and J.P. Petit, ''Heat Transfer,'' Prentice Hall, London (1993).

38 J. E. Andrew, P. E. Dyer, D. Forster, and P. H. Key, *Appl. Phys. Lett.*, **43**, 717 (1983).

39 J. H. Brannon, J. R. Lankard, A. I. Baise, F. Burns, and J. Kaufman, *J. Appl. Phys.*, **58**, 2036 (1985).

40 H. Fukumura, N. Mibuka, S. Eura, and H. Masuhara, *Appl. Phys. A*, **53**, 255 (1991).